

**MICROSTRUCTURAL INVESTIGATION OF SINTERED Nd<sub>16</sub>Fe<sub>76</sub>B<sub>8</sub> IID MAGNETS**

R. N. Faria, H. Takiishi, L. F. C. P. Lima,

*Instituto de Pesquisas Energéticas e Nucleares IPEN - CNEN/SP.*

X.J. Yin and I.R. Harris

*School of Metallurgy and Materials, University of Birmingham, U.K.*

The magnetic properties of Nd-Fe-B type magnets are determined not only by the high magnetocrystalline anisotropy of hard magnetic matrix phase (Nd<sub>2</sub>Fe<sub>14</sub>B) but also by the microstructure of the materials. In a previous work<sup>1</sup>, the microstructure of an alloy with a composition of Nd<sub>16</sub>Fe<sub>76</sub>B<sub>8</sub> has been investigated using scanning electron microscopy (SEM). The microstructure of this as-cast alloy has shown to be columnar in nature and the majority phase was the Nd<sub>2</sub>Fe<sub>14</sub>B ( $\phi$ ) phase surrounded by Nd-rich phase and Nd<sub>1+c</sub>Fe<sub>4</sub>B<sub>4</sub> boride phase. In the present work, the microstructure of a sintered Nd<sub>16</sub>Fe<sub>76</sub>B<sub>8</sub> magnet produced by the hydrogen decrepitation (HD) process<sup>2</sup> has been investigated using scanning electron microscopy (SEM) and transmission electron microscopy (TEM). The demagnetization curves of this HD magnet are shown in Ref. 1 (Br=12.26±0.01kG, iHc=12.72±0.03kOe, bHc=11.31±0.06kOe, BHmax=38.24±0.21 MGOe, Squareness factor = 0.90 and density=7.46g/cc).

The microstructure of this HD magnet studied by SEM reveal a morphology consisting of the majority Nd<sub>2</sub>Fe<sub>14</sub>B matrix grains, the boron-rich phase (Nd<sub>1+c</sub>Fe<sub>4</sub>B<sub>4</sub>) and the Nd-rich phase (as in the case of the as-cast Nd<sub>16</sub>Fe<sub>76</sub>B<sub>8</sub> alloy but with a very fine grain size). Very occasionally, there were some randomly distributed (Nd) oxide precipitates in the matrix phase grains. Fig. 1 shows the TEM investigated region of this phase. These oxides also occurred at the boundaries between the matrix grains and the boron-rich grains and this is shown in fig. 2. It has been suggested<sup>3</sup> that the precipitates are Nd<sub>2</sub>O<sub>3</sub>, formed before the sintering process and originated from impurities of the starting material. These large oxides could act as nucleation centres for magnetization reversal.

Quantitative conventional EDX microanalyses of the matrix phase, the boron-rich phase and the Nd-rich region led to compositions of ~13.7at%Nd, ~86.3at%Fe ; ~23.7at%Nd, ~76.3at%Fe and 95~98at%Nd, 2~5at%Fe respectively. The capability of WDX spectrometry for light element analysis is somewhat limited by its low spatial resolution. It is very difficult or even impossible for the electron probe beam to resolve down to 1  $\mu\text{m}$ . Furthermore, the volume of the sample which contributes to the X-ray signal is relatively independent of the size of the electron probe because high angle elastic scattered electrons within the sample generate X-rays. These factors together limit the application of WDX in obtaining further information from the Nd-rich and boron-rich boundary phases along the grain boundaries in a sample which has a very fine grain size<sup>4</sup>.

It is widely accepted that the grain boundaries play an important role in the coercivity mechanism of the sintered Nd-Fe-B type magnets. TEM observations indicated that a large number of Nd<sub>2</sub>Fe<sub>14</sub>B-Nd<sub>2</sub>Fe<sub>14</sub>B grain boundaries appeared to be without any Nd-rich thin layers along them. The only evidence for the existence of the Nd-rich phase layers in such a Nd<sub>2</sub>Fe<sub>14</sub>B-Nd<sub>2</sub>Fe<sub>14</sub>B grain boundary region came from compositional analyses showing a higher Nd concentration (see fig. 3 and table 1). High resolution microanalysis was conducted in a VGHB501 microscope using a nominal probe size of 2nm. Compositional profiles across the  $\phi$ - $\phi$  interfaces were obtained by manual placement of the probe followed by acquisition and quantification of the spectra. The interface regions have higher Nd than the surrounding Nd<sub>2</sub>Fe<sub>14</sub>B matrix grains.

## References

- <sup>1</sup>R. N. Faria, H. Takiishi, L. F. C. P. Lima, X.J. Yin and I.R. Harris, XIV Colóquio da Sociedade Brasileira de Microscopia Eletrônica., Caxambu, Vol 3 (1993) 69
- <sup>2</sup>Harris I. R., J. Less-Common Metals 131 (1987) 245
- <sup>3</sup>J. Fidler, IEEE Trans. Mag., MAG-23, (5) (1987) 2106
- <sup>4</sup>X. J. Yin, M. G. Hall, I. P. Jones, R. N. Faria and I.R. Harris, J. Magn. Mater, 125 (1993) 78





**Fig.1** TEM micrograph showing a large Nd<sub>2</sub>O<sub>3</sub> oxide within a matrix grain.



**Fig.2** TEM micrograph showing large Nd<sub>2</sub>O<sub>3</sub> oxides at a boundary between the matrix and the boron-rich grain.

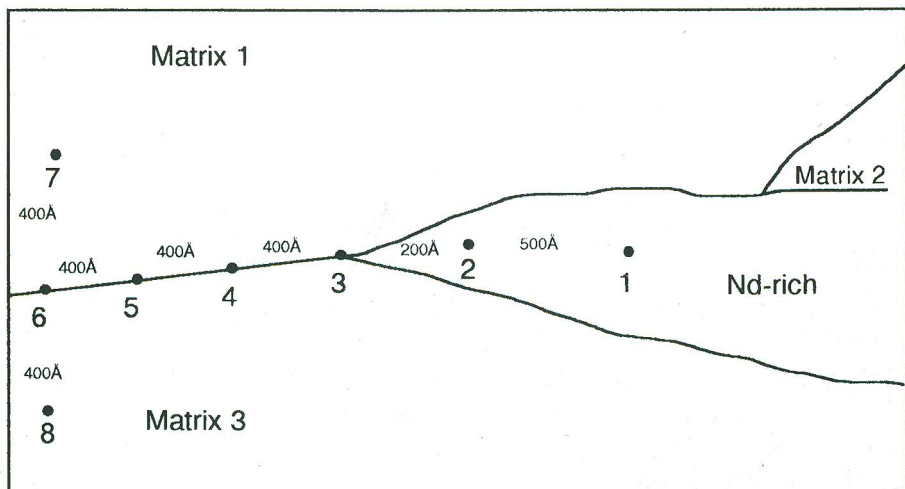


**Fig.3** Schematic of TEM micrographs showing  $\text{Nd}_2\text{Fe}_{14}\text{B}$ - $\text{Nd}_2\text{Fe}_{14}\text{B}$  grain boundaries apparently without any Nd-rich phase.

**Table 1.** High resolution microanalyses (2nm) showing a higher Nd concentration along the  $\text{Nd}_2\text{Fe}_{14}\text{B}$ - $\text{Nd}_2\text{Fe}_{14}\text{B}$  grain boundary regions, apparently without any Nd-rich phase, than in the surrounding matrix grains.

Spectra No.	Nd (at%)	Fe (at%)	Error bar
1	39.20	60.80	0.60
2	30.45	69.55	0.52
3	32.83	67.17	0.54
4	23.12	76.88	0.49
5	23.02	76.98	0.47
6	14.46	85.54	0.37
7	14.72	85.28	0.36
8	14.94	85.06	0.42